International Journal of Enhanced Research in Science, Technology & Engineering
ISSN: 2319-7463, Vol. 11 Issue 12, December-2022, Impact Factor: 7.957

Monitoring of Low-Cost Three-Phase Four-Switch Inverter-Fed Drives for Applications with Brushless DC Motors

Dr. M. Sangeetha[1], Mr. S. Ajith[2], Mr. G. Purusothman[3]

[1]Professor, Electrical and Electronics Engineering, MAM School of Engineering
[2]PG Student, Electrical and Electronics Engineering, MAM School of Engineering
[3]Assistant Professor, Electrical and Electronics Engineering, MAM School of Engineering

ABSTRACT

This work proposes an efficient control method for Brushless DC Motor (BLDCM) drives with trapezoidal back Electromotive Force (EMF) provided by three-phase, four-switch inverters. In the suggested method, the inner control loop based on a hysteresis controller governs the BLDC phase currents while the outer control loop for regulating the motor speed is constructed using Model Predictive Control (MPC). Effective switching strategies for the motor and generator modes are proposed to efficiently adjust the current of the uncontrolled phase in the four-switch inverter. The proposed control strategy optimizes the speed transient response in terms of tracking error and speed overshoot/undershoot while achieving favorably reduced torque ripples It might be the best choice for applications requiring cheap, low-power BLDCM. Additionally, to reduce the real-time computational burden, a suitable cost function is solved offline and used to tune the MPC-based speed control loop. It is demonstrated using the aforementioned method that the proposed MPC-based controller can be implemented with the same ease as the PI controller while still providing superior control performance. The suggested BLDCM drive system is experimentally tested using a 1200W BLDCM and dSPACE1104 development board in a Hardware-in-the-Loop (HiL) test configuration. The outcomes of the experiments show how the suggested drive mechanism is advantageous.

Index Terms— **Hysteresis control, brushless DC motor (BLDCM), four-switch inverter-fed motor drives, Hardware-in- the-Loop, model predictive control.**

INTRODUCTION

Brushless Dc Motors (BLDCMs) have come to dom-inate a wide range of applications including household appliances, small electric bikes, motion control systems, etc.[1], [2]. The superiorities of the BLDCMs mainly includehigher power density, higher efficiency, and longevity of these machines compared to their brushed counterparts. The common method for driving the three-phase BLDCMs is to usethree-phase Six-Switch Voltage Source Inverters (SSVSIs) [3]. Alternatively, three-phase Four-Switch Voltage Source Invert-ers (FSVSIs) with special control mechanisms have been used to drive the BLDCMs [4]–[18]. In the FSVSI, one leg of the three-phase SSVSI is substituted by two common series- connected capacitors and one motor terminal is connected to the center tap of these capacitors. Thus, due to the elimination of two semiconductor switches and related gate drive circuitry,the overall implementation cost would be reduced, which makes the FSVSI a favorable choice for low-power BLDCM drives.

Nonetheless, in the FSVSI-based BLDCM drive, one of the phases becomes uncontrollable which may lead to fluctuations in the center tap voltage of the capacitors and unbalance among the BLDCM phase currents. Such conditionscan potentially increase the torque ripples and in the worst caselead to a failure in the drive system. Therefore, for FSVSI- based BLDCM drives, it is necessary to adopt efficient control strategies for minimizing the torque ripple and ensuring that the speed/current transient responses are not too harsh to cause control loop instability and damage to the weak FSVSI system. To this end, several approaches have been proposed in the literature, which all are briefly reviewed in the following:

The feasibility of using FSVSI for low-cost BLDCM drives was first evaluated by Lee and Ehsani in [4]–[6], where direct current controlled pulse wide modulation (PWM) was used together with an efficient switching strategy for minimizing the torque ripple of the BLDCM. Several other research works have so far been proposed for controlling the FSVSI-fed

BLDCMs. In [7], an effective compensation scheme for reduc- ing the current imbalance caused by the capacitive impedancesof the uncontrolled phase of the FSVSI-fed motor drives has been proposed. The main idea of this work is to add similar virtual capacitive impedances to the terminals of the controlled phases for balancing the three-phase system. In [8], a current reference generation scheme has been proposed for space vector PWM (SVPWM)-based FSVSI-fed BLDCM drives to reduce the torque ripple during current commutations.In [9], a comprehensive analysis of low-frequency and high- frequency torque ripples in the SVPWM-based FSVSI-fed drives has been carried out. Additionally, a simple compen- sation scheme based on the introduction of non-orthogonal. Additionally, an efficient switching template based on thevoltage vector look-up table has been proposed to produce the desirable torque characteristics. To further improve the cost- effectiveness of the FSVSI-fed BLDCM drives, an effective control strategy that uses only one current sensor has been proposed in [14]. In the control scheme proposed in [14], only the current waveform of the uncontrolled phase is measured and directly used to control the respective phase current duringits activation periods.

Coordinate transformation has also been proposed to minimize the torque ripples. Minimization of the torque ripples in FSVSI-fed drives has also been discussed in [10], where a hybrid SVPWM method based on using two zero vector synthesis approaches during each fundamental period has been proposed. In [11], two SVPWM approaches for the FSVSI-fed drives have been proposed to suppress the zero-sequence volt- age/current. In the current control scheme proposed in [12], two regulating vectors have been added to each control cycle of the conventional PWM scheme for regulating the current of the uncontrolled phase by controlling the activation time of the regulating vectors. The application of the direct torque control (DTC) for BLDCMs driven with FSVSI has been proposed in [13]. In this work, the required quasi-square current waveforms are obtained by selecting the voltage space vectors from a simple look-up table at a predefined sampling time. Additionally, an efficient switching template based on the voltage vector look-up table has been proposed to produce the desirable torque characteristics. To further improve the cost- effectiveness of the FSVSI-fed BLDCM drives, an effective control strategy that uses only one current sensor has been proposed in [14]. In the control scheme proposed in [14], only the current waveform of the uncontrolled phase is measured and directly used to control the respective phase current during its activation periods. When the uncontrolled phase is at rest, the current regulation is accomplished by analytically deriving different rules that affect the uncontrolled phase current during the rest periods. To further reduce the implementation cost of the FSVSI-fed BLDCM drive, the feasibility of eliminating the Hall effect sensors by using sensorless control techniques have also been successfully verified in [15]–[17]. In all the control schemes reviewed before, simple PI controllers have been used to control the speed of the FSVSI-fed BLDCM. However, the use of the PI controller is not efficient especially in FSVSI-based applications where an aggressive speed transient response can cause intolerable transient conditions for the weak FSVSI-based drive. Therefore, apart from efficient con- trol of the current loop, the speed control loop should also have a good performance. To achieve this goal, in [18], the fuzzy logic-based controller has been proposed to adjust the speed of the motor equipped with FSVSI, where excellent performance characteristics in terms of the speed overshoot/undershoot and steady-state tracking error have been obtained. However, it is often tedious to develop the required fuzzy rules and member- ship functions. Also, developing a fuzzy system requires a lot of data and expertise.

The usefulness of Model Predictive Control (MPC) for controlling FSVSI-based Permanent Magnet Synchronous Motor (PMSM) drives have been discussed in [19], [20]. In [19], a simplified MPC without weighting factors is for- mulated to control the motor flux, where the capacitor voltage offset is also suppressed using a stator flux compensator. The MPC-based flux control of FSVSI-based flux-reversal perma- nent magnet (FRPM) motor drives has also been discussed in [20]. However, in these works, the MPC has been used for controlling the motor flux and the speed loop is adjusted using the traditional PI controllers. In this paper, an efficient control strategy for FSVSI-fed BLDCMs is proposed. In the proposed control scheme, the outer speed control loop is realized using Model Predictive Control (MPC), which helps to achieve a superior speed transient response. The MPC generates optimum references for the motor phase currents, which are subsequently fed to the inner current control loop based on the hysteresis control mechanism. Besides, efficient switching patterns for current control at both motor and generator modes are developed, which substantially reduce the BLDCM torque ripple during motor and generator modes. Thecontributions of this paper are explicitly listed as follows:

1- This work is the first attempt for predictive speed control ofthe FSVSI-fed BLDCMs. In comparison with the existing methods, The proposed scheme provides a superior speed transient response.
2- The control law of the proposed MPC controller is obtained in an offline manner, which significantly improves the computational efficiency. It is also mathematically shown that the implementation of the proposed MPC controller becomes as simple as a PI controller.
3- In comparison with other methods that discuss only the motor mode, the switching patterns and current control for the generator mode are developed, as well.

The rest of the paper is structured as follows. In Section II, the problem of controlling the BLDCM with FSVSI structure is

discussed in more detail. In Section III, the operating principles of the proposed approach including the MPC-based speed controller, switching patterns, and hysteresis current controller are discussed. To demonstrate the effectiveness of the proposed control scheme, the HiL experimental results are provided and discussed in Section IV. Section V provides comparative results between the proposed method and some other approaches. Finally, in Section VI, the concluding remarks areprovided.

FSVSI-BASED BLDCM CONTROL:PROBLEM STATEMENT

As shown in Fig. 1, the BLDCM produces trapezoidal back-Electromotive Force (EMF). Therefore, to generate constant output torque, the motor phase currents must necessarily have quasi-square waveforms synchronized with the three-phase back-EMFs. To achieve this, the phase currents must have 120° conducting and 60° non-conducting working regions during each half cycle of the motor electrical frequency. Likewise, at each instant, only two motor phases are active and the third phase current is zero. The required wave-forms for proper operation of the BLDCM during motor and generator operation modes are shown in Fig. 1. The wave- forms of Fig. 1 can be straightforwardly realized using the SSVSI structure with conventional PWM strategies. However,obtaining the quasi-square current waveforms of Fig. 1 using the FSVSI topology is challenging. The structure of the FSVSI-fed BLDCM is depicted in Fig. 2. As seen, since inthe FSVSI two power switches are replaced by two capacitors,Phase C current can no longer be directly controlled. Taking the motor operation mode (upper figure of Fig. 1) as an example, in operating modes 1, 3, 4, and 6, Phase C current can be indirectly controlled by appropriate switching of S_4,

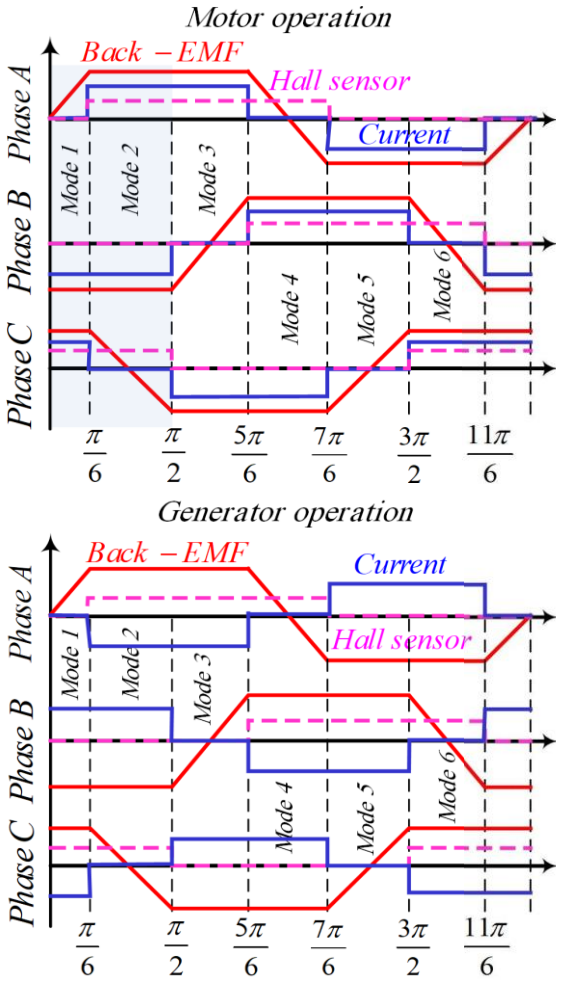

Fig. 1. Three-phase back-EMFs, current waveforms, and Hall effect signals of the BLDCM during one cycle of the motor electrical frequency under motorand generator operating modes.

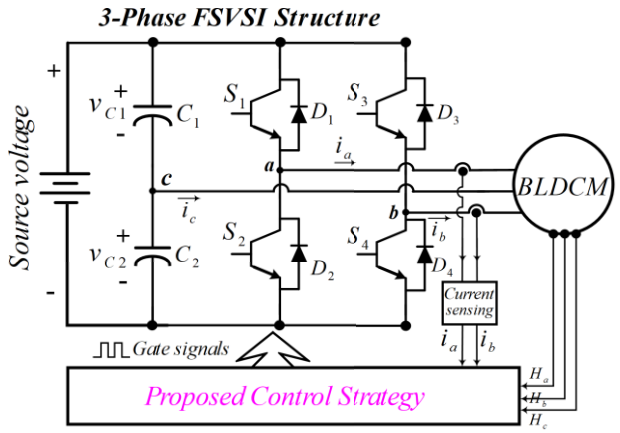

Fig. 2. Schematic of the FSVSI-fed BLDCM.

S_1, S_3, and S_2, respectively. However, during the operating modes 2 and 5, Phase C current cannot be set to zero with the traditional PWM strategy due to the fluctuations of the center tap voltage of the capacitors. Thus, during the rest periods related to modes 2 and 5, Phase C current continues to flow, which causes current imbalance and torque pulsation. Thus, an efficient control scheme must be adopted to rec-tify the problem associated with the uncontrolled Phase C.

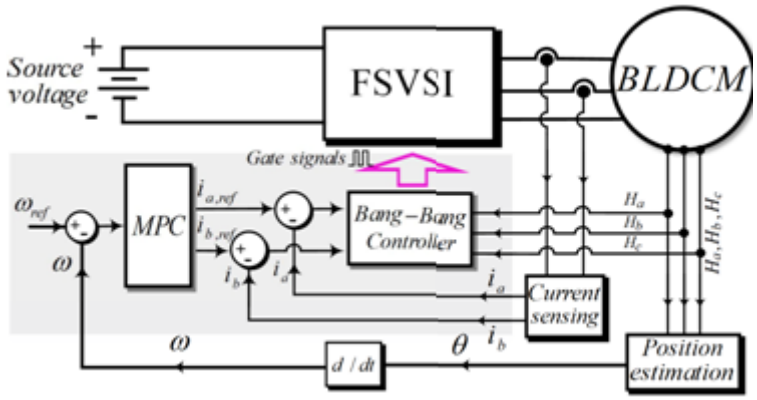

Fig. 3. Overview of the proposed control strategy for FSVSI-fed BLDCM.

Under the conditions explained above, the proper operation of the outer speed control loop also gains more importance because harsh transient responses might aggravate the voltage variations at the midpoint of the capacitors leading to instability of the speed control loop [21]. In the next section, and efficient strategy for FSVSI-fed BLDCM control is proposed.

OPERATING PRINCIPLES OF THE PROPOSED CONTROL SCHEME

The structure of the proposed control scheme for the FSVSI-fed BLDCM is shown in Fig. 3, in which the gate signals of the FSVSI are considered as the control vari- ables and speed of the BLDC motor is considered as the controlled variable. The motor speed is estimated using the low-resolution Hall effect sensors H_a, H_b, and H_c. As seen in Fig. 1, the status of Hall signals overall change six times (with $\pi/3$ phase shift) during each cycle of the motor electrical frequency. Thus, the motor speed can be easily estimated as follows:

$$\omega = \frac{\pi/3}{\Delta t} \times \frac{2}{P} = \frac{2\pi}{3P\Delta t} \qquad (1)$$

where ω is the motor speed in *rad/s*, P is the number of poles, and Δt is the measured time interval of $\pi/3$ periods. The motor speed ω is compared to its reference value ω_{ref} (ω) and the control error is fed to the speed controller. In the proposed control scheme, the MPC controller is used for realizing the outer control loop (speed loop). The speed control loop generates suitable references $i_{a,ref}$ and $i_{b,ref}$ for the controllable motor phase currents. Besides, the current regulation is

realized using an inner control loop based on the hysteresis controller together with efficient switching tem-plates for motor and generator operation modes. As will be demonstrated, the proposed control scheme provides superior transient response during speed or torque changes. Also, similar to conventional control methods, the proposed method uses two current sensors and three built-in Hall effect sensor signals, and thus, no hardware extension is required. The detailed procedure for designing the speed and current control loops are provided in the following subsections.

A. Design of the MPC-Based Speed Control Loop

It is well-known that the hysteresis controller has a very fastresponse. Also, the electrical time constant of the BLDCM

Table I: Switching Patterns For Current Regulation Using The FSVSI

Mode*	$H_aH_bH_c$	Active Phases	Silent Phase	Switches (motor)	Switches (generator)
1	001	B, C	A	S_4	S_3
2	101	A, B	C	S_1 and S_4	S_2 and S_3
3	100	A, C	B	S_1	S_2
4	110	B, C	A	S_3	S_4
5	010	A, B	C	S_2 and S_3	S_1 and S_4
6	011	A, C	B	S_2	S_1

*Operating modes are depicted in Fig. 1

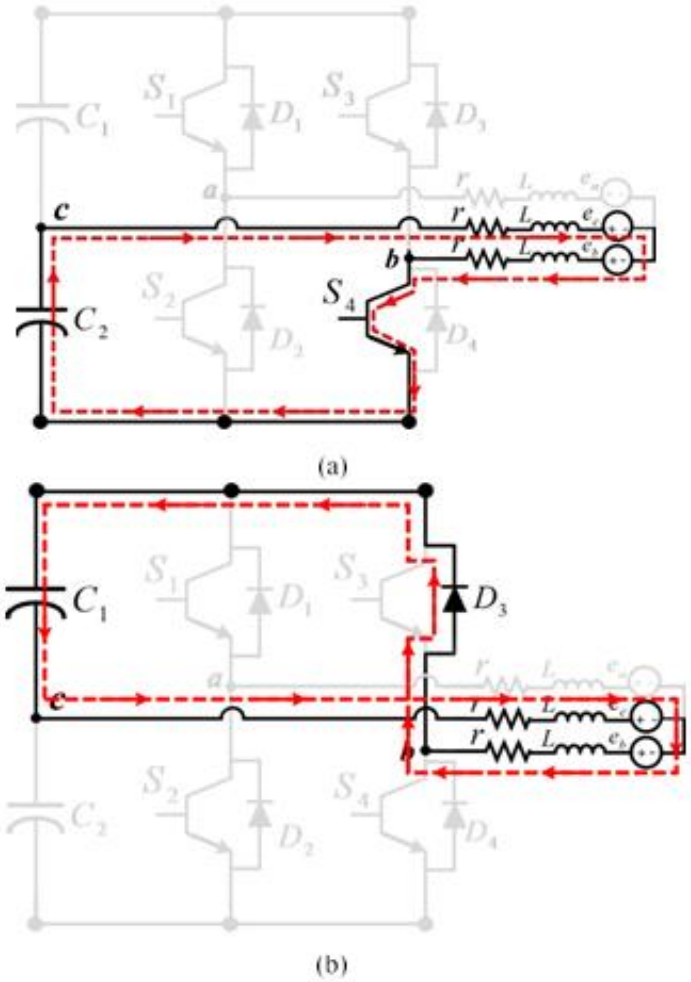

Fig. 4. Current flow during mode 1 of the utilized hysteresis current controller(motor operation). (a) S4 is turned on and D3 is deactivated (b) S4 is turned off and D3 is activated.

Control loop generates the reference currents for the innercurrent control loop. The use of the fast hysteresis controller thus helps to finish the inner control objective before the next control input generated by the outer loop is receivedat the next sample time. With hysteresis controller, smaller overshoots/undershoots can also be achieved, which reduces the torque ripples of the motor. Due to the space limitation, the operating modes 1 and 2 (refer to Fig. 1) during the motor mode are considered as examples to explain the working principles with more details. Assume I_{ref} and ε being the reference current command gen- erated by the proposed MPC-based speed control loop and the hysteresis controller band, respectively. In mode 1 of the motoroperation mode, switch A is deactivated making Phase A current equal to zero (I_a 0*)*. In this mode, the currents of active Phases B and C are controlled by switching of S_4. It should be noted that in this mode, as seen in Fig. 1, Phases B

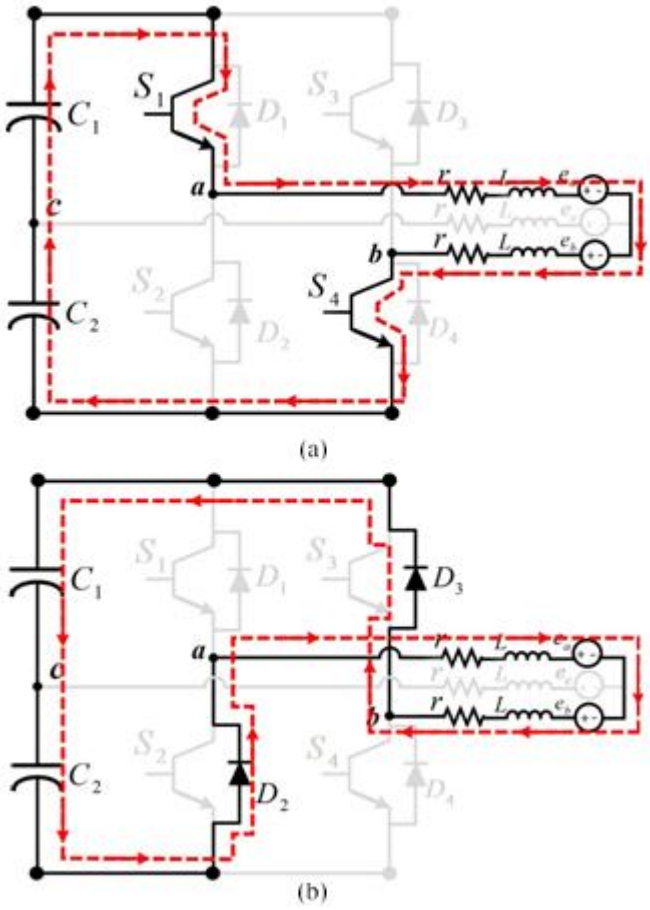

Fig. 5. Current flow during mode 2 of the utilized hysteresis current controller(motor operation). (a) S1 and S4 are turned on (b) S1 and S4 are turned off and current flow is automatically directed toward D2 and D3.

And C have negative and positive current values, respectively, i.e. $I_b < 0$, $I_c > 0$. Whenever $I_b \geq I_{ref} - \varepsilon$ and $I_c < I_{ref} + \varepsilon$ the currents of Phases B and C should be increased to the reference current command. To this end, switch S_4 is turnedon by the hysteresis controller. Fig. 4(a) shows the current paths in the FSVSI in this situation. As seen, when S_4 is turned on, the currents of Phases B and C are increased as aresult of discharging capacitor C_2. The absolute phase currentssteadily increase until the conditions $I_b \leq I_{ref} - \varepsilon$ and $I_c \geq I_{ref} + \varepsilon$ are satisfied. As soon as the foregoing conditions are met, switch S_4 is turned off, which puts D_3 in the forward bias state and thus, the phase currents are reduced through charging capacitor C_1, as seen in Fig. 4(b). The foregoing procedure is repeated during each operating mode to maintain the phase current within the hysteresis control band. The sameprinciple of mode 1 can be used for other operating modes. In mode 2, Phases A and B are active ($I_a > 0$, $I_b < 0$) and Phase C is silent ($I_c = 0$). Whenever $I_a < I_{ref} + \varepsilon$ and $I_b > I_{ref} - \varepsilon$, power switches S_1 and S_4 are turned on to increase the phase currents by discharging the split capacitors C_1 and C_2 to Phases A and B windings, as depicted in Fig. 5(a). The absolute values of the currents I_a and I_b continue to increase until the phase currents I_a and I_b reach the upper and lower limits of the control band, respectively,
i.e. when $I_a \geq I_{ref} + \varepsilon$ and $I_b \leq I_{ref} - \varepsilon$. Then, the switches S_1 and S_4 are turned off, which diverts the paths of the phase

currents to D_2 and D_3. Under such circumstances, as seen in Fig. 5(b), the magnitudes of the phase currents are reduced through charging the capacitors C_1 and C_2. Consequently, by turning on and off the switches S_1 and S_4, the increase and decrease of the phase currents can be controlled, which makes it possible to regulate the phase currents within a small controlband around the reference current trajectory.

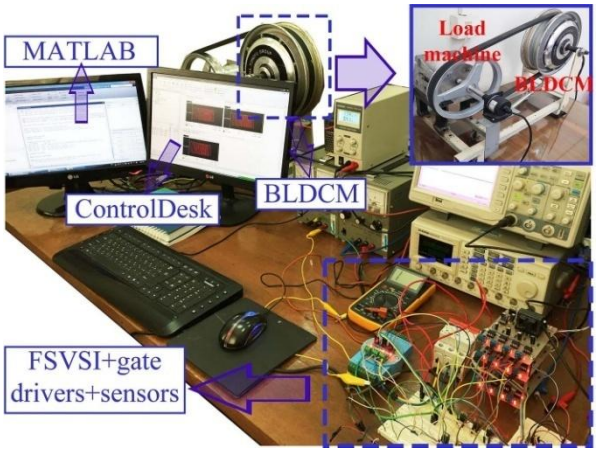

Fig. 6. Implemented HiL test setup.

It should be mentioned that a smaller control band ε reducesthe torque pulsations. However, if the control band is too small, the switching frequency increases, which gives rise to the switching losses. Thus, the selection of the controlband in the utilized hysteresis controller should be made by a trade-off between the levels of the torque ripple and switching losses. With regards to the control modes 2 and 5, it should also be noted that the current of the uncontrolled Phase C might become nonzero (due to the non-zero back-EMF of Phase C and absence of the controllable power switches) and cause unwanted current distortions. To resolve this problem, the switching of the power switches is fulfilled, indepen- dently [6]. Therefore, the hysteresis controller is independentlyimplemented for each operating mode of Table I. The active operating mode can easily be decided by monitoring of Hall effect sensors $H_aH_bH_c$, which have a unique status during eachoperating mode, as shown in the second column of Table I.

HARDWARE-IN-THE-LOOP TEST RESULTS AND DISCUSSIONS

To evaluate the performance of the proposed approach, several experiments are conducted on the implemented HiL test setup and the obtained results are provided and discussed in this section. In the following, the implemented HiL setup and the experimental results are discussed with details.

A. Description of the HiL Test Setup

The implemented Hil test setup is shown in Fig. 8. The HiL setup mainly comprises a motor-generator set equipped witha 1.2kW BLDCM coupled with a 1.5kW Permanent Magnet Synchronous Motor (PMSM) using a coupling belt with almost 1:1 speed ratio. Therefore, since the rating of the loading machine is higher than the under-study BLDC motor, the test motor can be loaded to its rated torque condition. The BLDCM and PMSM are controlled with custom-made small prototypes of the FSVSI and SSVSI, respectively. The current waveforms are measured using ACS712ELCTR-30A-T Hall effect-based linear current sensors from Allegro©. Also, the BLDCM speed is estimated with the aid of three built-in Hall effect-based position sensors using (1). The generated gate commands sig- nals are fed to the FSVSI through isolated gate drive circuitry with A3120 gate drivers. All the control units including the proposed speed and current controllers as well as control of the PMSM are implemented in MATLAB/SIMULINK. The dSPACE1104 platform is used for controlling the HiL setup. The implemented controllers are compiled using MATLAB's CODER option and the built description file is used in dSPACE ControlDesk experiment software, which enables real-time control, monitoring, and data-logging, simultane- ously. The current waveforms are recorded using Tektronix MSO5054 digital oscilloscope. The speed waveforms are first recorded as MATLAB's standard files and are then used for plotting in MATLAB. The sampling time of the description file, hysteresis controller, and MPC controller are set to 100μs. Detailed information on the HiL test setup and the BLDCM is provided in Table II. In the following subsection, the exper- imental results are provided and discussed.

Table II: Experimental Parameters

Parameter	Value
BLDCM	1.2kW, 72V hub motor
Loading Machine	1.5kW, 48V PMSM
Control Board	dSPACE1104 platform
Current Sensors	ACS712ELCTR-30A-T
T_s	100 μs
$MPC\ horizons$	N_p =2 , N_c = 1
Control band ε	0.5
Weighting Factors	$\delta = 0.7, \lambda = 0.3$
P	4
J	0.0012 kg.m^2
B	0.001 N.m.s

B. Experimental Results

The performance of the proposed control scheme is inves- tigated through several experiments under different operating conditions. In Fig. 7, the steady-state three-phase BLDCM cur-rents, three-phase Hall effect signals, as well as the switching signals of the FSVSI under load torque of 2 Nm and rotational speed of 600 rpm are shown. As seen, the quasi-square current waveforms are successfully constructed using the current con- troller based on hysteresis control. It is evident that during the rest modes of Phase C (modes 2 and 5), the controller suitably adjusts the current around almost zero. Overall, Fig. 7 shows that based on Fig. 1 and switching sequences of Table I, the waveforms are constructed exactly as expected. The con- troller performance can further be improved by reducing the control band, which would be obtained at the cost of slightly higher switching frequency and losses. Fig. 8 shows the experimental waveforms of the proposed method in generator mode. Similar to the motor mode, the quasi-square current waveforms are successfully constructed in the generator mode using the proposed strategy of Table I. In the conventional

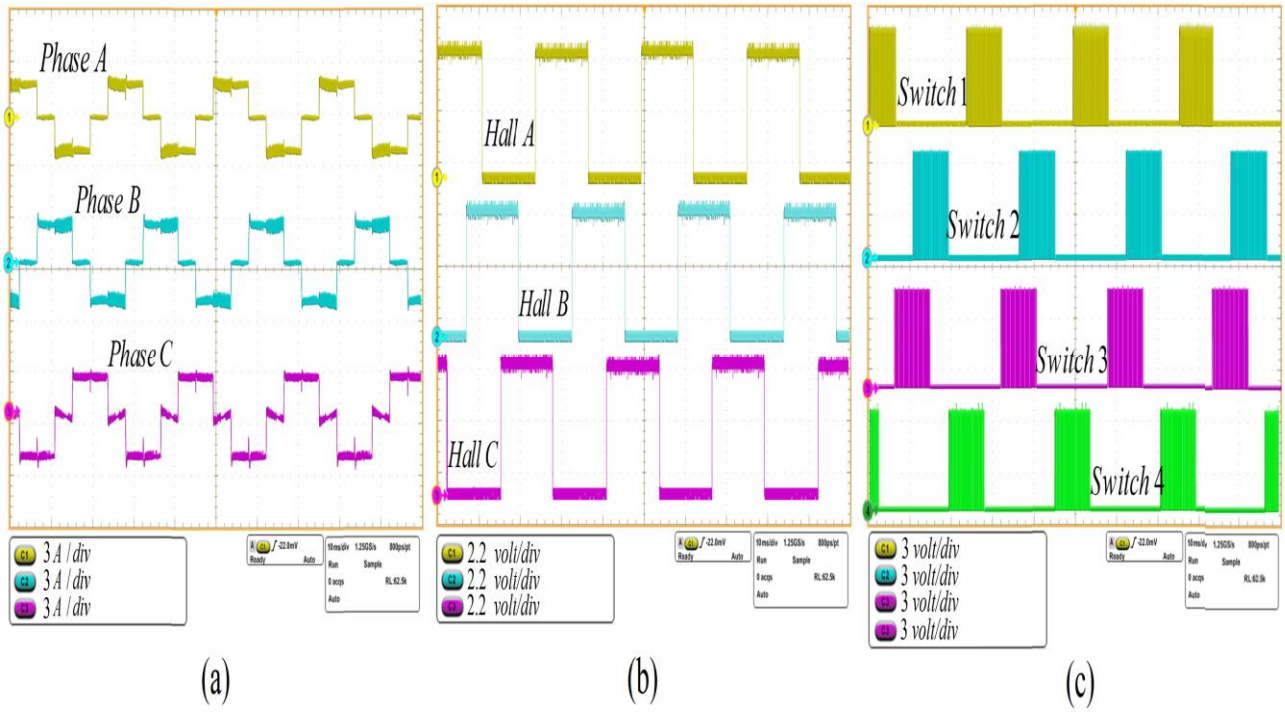

Fig. 7. Experimental waveforms in the steady-state conditions when the BLDCM works in the motor mode and is loaded by 2 Nm of the rated load torque and rotates at 600rpm. (a) Three-phase BLDCM phase currents. (b) Three-phase Hall effect signals. (c) Switching signals S1 to S4.

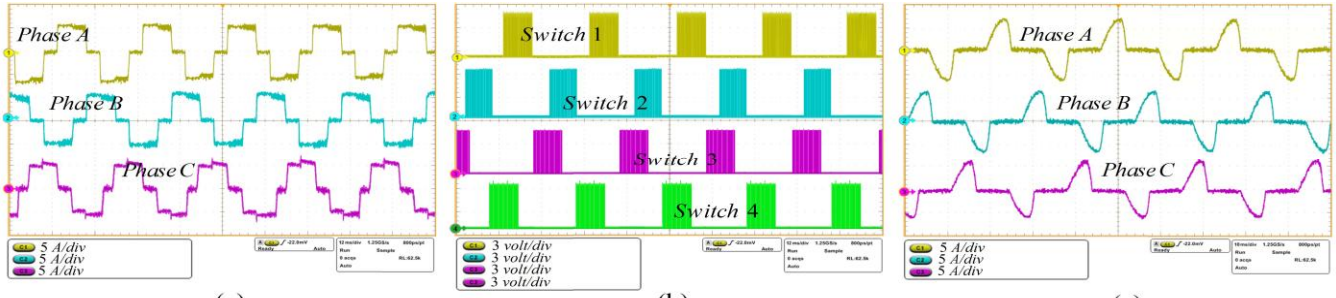

Fig. 8. Experimental waveforms in the steady-state conditions when the BLDCM operates in the generator mode and rotates at 600rpm. (a) Three-phase BLDCM phase currents with using the proposed switching strategy. (b) The switching signals S1 to S4 in the same time interval of Fig. 9(a). (c) Three-phase BLDCM phase currents without using the proposed switching strategy.

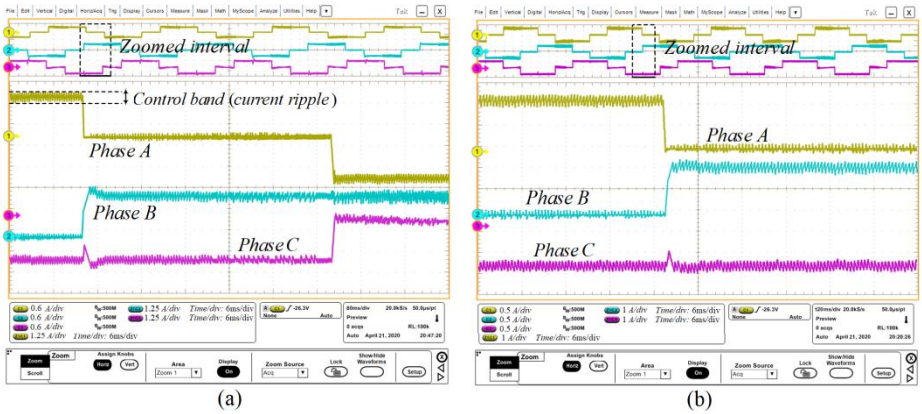

Fig. 9. Zoomed three-phase current waveforms of the BLDCM at different rotational speeds. (a) 1200 rpm (b) 800 rpm.

Scheme, the energy released during the generator mode canbe transmitted to the DC-link through conduction of anti-parallel diodes of the IGBTS, which will result in the current waveforms of Fig. 8(c). However, due to the trapezoidal back-EMFs of the BLDCM, such current waveforms will cause pulsative regenerative (braking) torque, which is not desirable. Using the proposed control strategy, a relatively smooth torque can be guaranteed during both the motor and generator modes. Fig. 7 shows the zoomed three-phase current waveforms under two different rotational speeds of 1200rpm and 800 rpm.

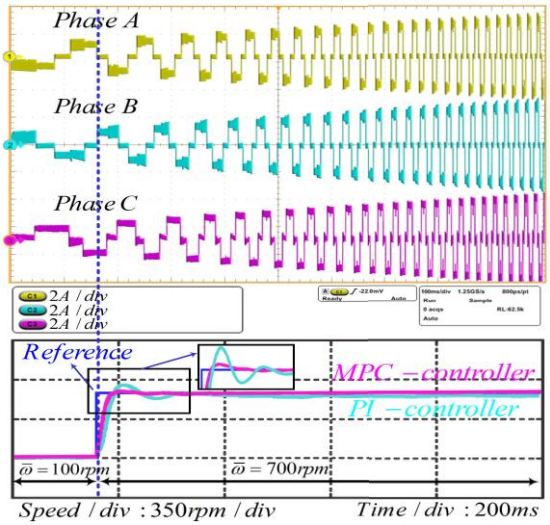

Fig. 10. Experimental waveforms under the speed change condition when the BLDCM speed is increased from 100rpm to 600rpm in a stepwise manner. Upper: Three-phase BLDCM phase currents. Lower: Speed responses of the proposed MPC-based controller and PI controller.

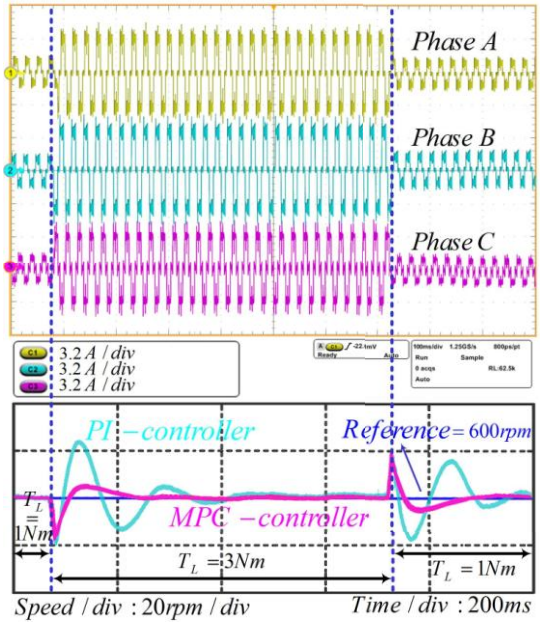

Fig. 11. Experimental waveforms under sudden step load changes from 1Nm to 3Nm and vice versa. Upper: Three-phase BLDCM phase currents. Lower: Speed responses of the proposed MPC-based controller and PI controller.

It is evident that in both cases, the phase currents are appro- priately regulated within the chosen control band of 0.5A. The current (torque) ripple can further be reduced by decreasing the band of the hysteresis controller. However, decreasing the controller band causes the phase current to reach the upper and lower bounds, more frequently. Therefore, a very low controller band can cause the excessive generation of heat dueto the switching losses of the IGBTs. In practice, the band of the current controller must always be limited to a suitable value. In Figs. 10 and 11, the dynamic performances of the proposed control scheme under transient speed change and transient load change conditions are shown. Fig. 10 shows the three-phase BLDCM phase currents and speed response when the BLDCM reference speed is increased from 100 rpm to 700 rpm in a stepwise manner. The current waveforms indicate the proper construction of the quasi-square current waveformsduring the speed change conditions. The speed response of theproposed MPC-based speed controller, as well as the compar- ison with the traditional PI controller, are shown in the lower plot of Fig. 10.

Table III: Comparison Between Different Speed Control Methods

	Rise time	Settling time*	Overshoot	Error**
PI [5]	~25 m.s.	~170 m.s.	~87 rpm	~ 10 rpm
Fuzzy-Logic [18]	~120 m.s.	~150 m.s.	<5 rpm	< 1 rpm
MPC (proposed)	~20 m.s.	~30 m.s.	<5 rpm	< 1 rpm

* 5% criterion (when speed settles within 5% of the steady-state value) * Steady-state error

The PI is tuned to provide its best performance in terms of transient overshoot, settling time, as well as the steady-state speed tracking error. The results suggest that the MPC and PI controllers both achieve a sufficiently small rise time below 20 milliseconds. However, the transient speed response with the PI controller shows a relatively big overshootreaching 50 rpm, which is not acceptable for the FSVSI- based BLDCM application. On the other hand, the speed overshoot with the MPC controller is favorably below 4 rpm making it superior to its counterpart. Also, the steady-state speed tracking error of <0.5rpm is achieved with the MPC controller, which is very advantageous in comparison with the steady-state error of the PI controller obtained about 3 rpm. Although the PI controller can potentially achieve a lower tracking error by increasing the coefficient of the integrator term this will give rise to the speed settling time, which is not desirable. Fig. 13 shows the experimental waveforms when two successive sudden step changes in the load torque from 1Nm to 3Nm and vice-versa take place. It is evident that beforethe occurrence of the load change both of the controllers have successfully tracked the reference speed 600rpm. However, the BLDCM speed experiences a rapid decrease by about20rpm when the load torque is suddenly increased to 3Nm. The speed response with the MPC controller shows that the speed successfully converges on the speed setpoint while it experiences a small overshoot with about 4 rpm. On the other hand, the speed response with the PI controller experiences two overshoot and undershoot of about 25 rpm and 15rpm, respectively. Besides, the settling time

of the MPC-controller is significantly lower than that of the PI controller. Likewise, during the second load torque change condition when the torque is suddenly reduced from 3Nm to 1Nm., the BLDCM speed suddenly diverges from its setpoint; however, the refer- ence speed is smoothly recovered using the proposed MPC- based control scheme. Similar to the first load change event, the speed response of the MPC excels the response of the PI controller in terms of the settling time and overshoot. Overall, the results demonstrate that the proposed method performs as designed and provides satisfactory performance characteristics, which makes it a rational candidate for low and medium-power BLDCM applications, where a limited amount of current harmonics can be tolerated. A few potential applications include but are not limited to the fan, pump,compressor, and spindle drives, small electric vehicles, bikes, and scooters.

COMPARISON WITH SIMILAR CONTROL METHODS

In this section, the performance of the proposed MPC-based control scheme is compared with the fuzzy-logic-based controller and PI controller in terms of the rise time, settling time (5% criterion), overshoot, and steady-state speed tracking error. The comparative tests are carried out by computer sim- ulations using MATLAB/SIMULINK software. The obtained results are summarized in Table III. The results clearly show the superiority of the proposed speed control method against the conventional PI controller. The proposed MPC-based con- troller also outperforms the fuzzy-logic-based controller in terms of the rise time and settling time.

CONCLUDING REMARKS

This research proposes a novel FSVSI-based BLDCM drive system. The proposed control strategy primarily consists of an outside speed control loop produced by MPC and an inner current control loop based on the hysteresis controller. The BLDCM's quasi-square current waveforms are effectively created by employing effective switching techniques for both generator and motor operation modes. The suggested speed controller performs better than the PI-based speed controller in terms of overshoots, undershoots, and setup time, which lessens the strain on the BLDCM drive's weak FSVSI-based motor. The MPC controller is implemented similarly to a PI controller in terms of simplicity because the required CF is solved offline.

ACKNOWLEDGMENT

The authors sincerely appreciate the financial support of Irans National Elites Foundation for carrying out this research.

REFERENCES

[1] F. Naseri, E. Farjah, and T. Ghanbari, “An efficient regenerative braking system based on battery/supercapacitor for electric, hybrid, and plug-in hybrid electric vehicles with BLDC motor,” *IEEE Trans. Veh. Technol.*, vol. 66, no. 5, pp. 3724–3738, May 2017.

[2] A. Loria, “Robust linear control of (chaotic) permanent-magnet syn- chronous motors with uncertainties,” *IEEE Trans. Circuits Syst. I, Reg. Papers*, vol. 56, no. 9, pp. 2109–2122, Sep. 2009.

[3] F. Naseri, E. Farjah, Z. Kazemi, E. Schaltz, T. Ghanbari, and J.-L. Schanen, “Dynamic stabilization of DC traction systems using a supercapacitor-based active stabilizer with model predictive control,” *IEEE Trans. Transport. Electrific.*, vol. 6, no. 1, pp. 228–240, Mar. 2020.

[4] B. K. Lee and M. Ehsani, “Advanced BLDC motor drive for low cost and high performance propulsion system in electric and hybrid vehicles,”in *Proc. IEEE Int. Electr. Mach. Drives Conf.*, Jun. 2001, pp. 246–251.

[5] B.-K. Lee, T.-H. Kim, and M. Ehsani, “On the feasibility of four-switch three-phase BLDC motor drives for low cost commercial applications: Topology and control,” *IEEE Trans. Power Electron.*, vol. 18, no. 1, pp. 164–172, Jan. 2003.

[6] B. K. Lee, T. H. Kim, and M. Ehsani, “On the feasibility of four-switch three-phase BLDC motor drives for low cost commercial applications: Topology and control,” in *Proc. IEEE Appl. Power Electron. Conf. Expo.*, vol. 1, Mar. 2001, pp. 428–433.

[7] J. Kim, J. Hong, and K. Nam, “A current distortion compensation scheme for four-switch inverters,” *IEEE Trans. Power Electron.*, vol. 24,no. 4, pp. 1032–1040, Apr. 2009.

[8] S.-H. Park, T.-S. Kim, S.-H. Ahn, and D.-S. Hyun, “A simple current control algorithm for torque ripple reduction of brushless DC motor using four-switch three-phase inverter,” in *Proc. IEEE Conf. Power Electron. Spec.*, vol. 2, Jun. 2003, pp. 574–579.

[9] C. Zhu, Z. Zeng, and R. Zhao, “Comprehensive analysis and reduction of torque ripples in three-phase four-switch inverter-fed PMSM drives using space vector pulse-width modulation,” *IEEE Trans. Power Electron.*, vol. 32, no. 7, pp. 5411–5424, Jul. 2017.

[10] Z. Zeng, C. Zhu, X. Jin, W. Shi, and R. Zhao, “Hybrid space vector modulation strategy for torque ripple minimization in

three-phase four- switch inverter-fed PMSM drives," *IEEE Trans. Ind. Electron.*, vol. 64, no. 3, pp. 2122–2134, Mar. 2017.

[11] W. Li, S. Xuan, Q. Gao, and L. Luo, "Investigation of a four-switch four-leg inverter: Modulation, control, and application to an IPMSM drive," *IEEE Trans. Power Electron.*, vol. 34, no. 6, pp. 5655–5666, Jun. 2019.

[12] C. Xia, D. Wu, T. Shi, and W. Chen, "A current control scheme of brushless DC motors driven by four-switch three-phase inverters," *IEEE*
J. Emerg. Sel. Topics Power Electron., vol. 5, no. 1, pp. 547–558, Mar. 2017.

[13] S. B. Ozturk, W. C. Alexander, and H. A. Toliyat, "Direct torque control of four-switch brushless DC motor with non-sinusoidal back EMF," *IEEE Trans. Power Electron.*, vol. 25, no. 2, pp. 263–271, Feb. 2010.

[14] C. Xia, Z. Li, and T. Shi, "A control strategy for four-switch three- phase brushless DC motor using single current sensor," *IEEE Trans. Ind. Electron.*, vol. 56, no. 6, pp. 2058–2066, Jun. 2009.

[15] C.-T. Lin, C.-W. Hung, and C.-W. Liu, "Sensorless control for four- switch three-phase brushless DC motor drives," in *Proc. IEEE Ind. Appl. Conf., 41t IAS Annu. Meeting*, Oct. 2006, pp. 2048–2053.

[16] C.-T. Lin, C.-W. Hung, and C.-W. Liu, "Position sensorless control for four-switch three-phase brushless DC motor drives," *IEEE Trans. Power Electron.*, vol. 23, no. 1, pp. 438–444, Jan. 2008.

[17] A. H. Niasar, A. Vahedi, and H. Moghbelli, "A novel position sensorless control of a four-switch, brushless DC motor drive without phase shifter," *IEEE Trans. Power Electron.*, vol. 23, no. 6, pp. 3079–3087, Nov. 2008.

[18] M. N. Uddin, T. S. Radwan, and M. A. Rahman, "Fuzzy-logic-controller- based cost-effective four-switch three-phase inverter-fed IPM synchro- nous motor drive system," *IEEE Trans. Ind. Appl.*, vol. 42, no. 1, pp. 21–30, Jan. 2006.

[19] D. Sun, J. Su, C. Sun, and H. Nian, "A simplified MPFC with capacitor voltage offset suppression for the four-switch three-phase inverter-fed PMSM drive," *IEEE Trans. Ind. Electron.*, vol. 66, no. 10, pp. 7633–7642, Oct. 2019.

[20] W. Hua, W. Huang, and F. Yu, "Improved model-predictive-flux-control strategy for three-phase four-switch inverter-fed flux-reversal permanent magnet machine drives," *IET Electr. Power Appl.*, vol. 11, no. 5, pp. 717–728, May 2017.

[21] H. Ren and D. Liu, "Nonlinear feedback control of chaos in permanent magnet synchronous motor," *IEEE Trans. Circuits Syst. II, Exp. Briefs*, vol. 53, no. 1, pp. 45–50, Jan. 2006.

[22] H. Yan, J. Han, H. Zhang, X. Zhan, and Y. Wang, "Adaptive event- triggered predictive control for finite time microgrid," *IEEE Trans. Circuits Syst. I, Reg. Papers*, vol. 67, no. 3, pp. 1035–1044, Mar. 2020.

[23] R. Morfin-Magaña, J. J. Rico-Melgoza, F. Ornelas-Tellez, and F. Vasca, "Complementarity model of a photovoltaic power electronic system with model predictive control," *IEEE Trans. Circuits Syst. I, Reg. Papers*, vol. 66, no. 11, pp. 4402–4414, Nov. 2019.

[24] A. Mohammadi, H. Asadi, S. Mohamed, K. Nelson, and S. Nahavandi, "Optimizing model predictive control horizons using genetic algorithm for motion cueing algorithm," *Expert Syst. Appl.*, vol. 92, pp. 73–81, Feb. 2018.

[25] Z. Kazemi, A. A. Safavi, S. Pouresmaeeli, and F. Naseri, "A practical framework for implementing multivariate monitoring techniques into distributed control system," *Control Eng. Pract.*, vol. 82, pp. 118–129, Jan. 2019.